



## Article

# Projecting the Impact of Climate Change on Runoff in the Tarim River Simulated by the Soil and Water Assessment Tool Glacier Model

Gonghuan Fang <sup>1,2,3</sup> , Zhi Li <sup>1</sup>, Yaning Chen <sup>1,\*</sup>, Wenting Liang <sup>1,4</sup>, Xueqi Zhang <sup>1</sup> and Qifei Zhang <sup>5</sup>

- <sup>1</sup> State Key Laboratory of Desert and Oasis Ecology, Key Laboratory of Ecological Safety and Sustainable Development in Arid Lands, Xinjiang Institute of Ecology and Geography, Chinese Academy of Sciences, Urumqi 830011, China; fanggh@ms.xjb.ac.cn (G.F.); liz@ms.xjb.ac.cn (Z.L.); liangwenting21@mails.ucas.ac.cn (W.L.); zhangxueqi19@mails.ucas.ac.cn (X.Z.)
- <sup>2</sup> Xinjiang Key Laboratory of Water Cycle and Water Utilization in Arid Zone of Xinjiang, Urumqi 830011, China
- <sup>3</sup> Sino-Belgian Joint Laboratory for Geo-Information, Urumqi 830011, China
- <sup>4</sup> University of Chinese Academy of Sciences, Beijing 100049, China
- <sup>5</sup> School of Geographical Sciences, Shanxi Normal University, Taiyuan 030031, China; 20210094@sxnu.edu.cn
- \* Correspondence: chenyn@ms.xjb.ac.cn; Tel.: +86-0991-782-3169

**Abstract:** Analyzing the future changes in runoff is crucial for efficient water resources management and planning in arid regions with large river systems. This paper investigates the future runoffs of the headwaters of the Tarim River Basin under different emission scenarios by forcing the hydrological model SWAT-Glacier using six regional climate models from the Coordinated Regional Downscaling Experiment (CORDEX) project. Results indicate that compared to the period of 1976–2005, temperatures are projected to increase by  $1.22 \pm 0.72$  °C during 2036–2065 under RCP8.5 scenarios, with a larger increment in the south Tianshan mountains and a lower increment in the north Kunlun Mountains. Precipitation is expected to increase by  $3.81 \pm 14.72$  mm and  $20.53 \pm 27.65$  mm during 2036–2065 and 2066–2095, respectively, under the RCP8.5 scenario. The mountainous runoffs of the four headwaters that directly recharge the mainstream of the Tarim River demonstrate an overall increasing trend in the 21st century. Under the RCP4.5 and RCP8.5 scenarios, the runoff is projected to increase by 3.2% and 3.9% (amounting to  $7.84 \times 10^8$  m<sup>3</sup> and  $9.56 \times 10^8$  m<sup>3</sup>) in 2006–2035. Among them, the runoff of the Kaidu River, which is dominated by rainfall and snowmelt, is projected to present slightly decreasing trends of 3–8% under RCP4.5 and RCP8.5 scenarios. For catchments located in the north Kunlun Mountains (e.g., the Yarkant and Hotan Rivers which are mix-recharged by glacier melt, snowmelt, and rainfall), the runoff will increase significantly, especially in summer due to increased glacier melt and precipitation. Seasonally, the Kaidu River shows a forward shift in peak flow. The summer streamflow in the Yarkant and Hotan rivers is expected to increase significantly, which poses challenges in flood risk management.

**Keywords:** climate change; CORDEX; runoff changes; trend prediction; Tarim River Basin



**Citation:** Fang, G.; Li, Z.; Chen, Y.; Liang, W.; Zhang, X.; Zhang, Q. Projecting the Impact of Climate Change on Runoff in the Tarim River Simulated by the Soil and Water Assessment Tool Glacier Model. *Remote Sens.* **2023**, *15*, 3922. <https://doi.org/10.3390/rs15163922>

Academic Editors: Adnan Rajib, Venkatesh Merwade and Zhu Liu

Received: 1 June 2023

Revised: 2 August 2023

Accepted: 5 August 2023

Published: 8 August 2023



**Copyright:** © 2023 by the authors. Licensee MDPI, Basel, Switzerland. This article is an open access article distributed under the terms and conditions of the Creative Commons Attribution (CC BY) license (<https://creativecommons.org/licenses/by/4.0/>).

## 1. Introduction

Global warming has caused changes in hydro-meteorological variables such as precipitation magnitude/patterns, accumulation and ablation of glaciers, and evapotranspiration, resulting in potential changes in runoff and the sustainable utilization of water resources [1–4]. For the alpine catchments, the runoff is recharged by glacier melt, snowmelt, and rainfall [5]. Their hydrological processes have strongly responded to recent climate change [6–8]. Quantifying the runoff change in the future is a major concern to water supply, ecosystems, hydropower, and human society, particularly in arid regions [9–11].

As is stated in IPCC reports [4], changes in mean and extreme streamflow are projected over most of the ice-free land surface. The streamflow is projected to increase with global warming in most regions, with considerable uncertainty in many catchments, especially

for those with scarce observations. At the global scale, Zhou et al. reported an increase in runoff, which was dominated by land surface changes [12]. Huss and Hock simulated the hydrological responses to climate change and glacier mass loss in 56 large-scale glacierized drainage basins using the GloGEM model [2]. Specially, regional investigations of future runoff changes are being conducted, especially for High Mountain Asia [8,11,13], including the Syr Darya and Amu Darya [1], the Ganges–Brahmaputra [14], the Indus, and others. These important projections provide significant insights into future changes in runoff.

The Tarim River originates from the surrounding Tianshan Mountains, the Kunlun Mountains, and the Pamir Plateau (Figure 1). The runoff is recharged by the glacier/snowmelt and rainfall and is highly sensitive to global warming. Due to the intensified water cycling, the processes of glacier melt and snowmelt have been altered, resulting in changes in mountainous runoff [5]. This poses a challenge to the livelihood of over 10 million people and the crops grown on 23,992.76 km<sup>2</sup> of agriculture land.

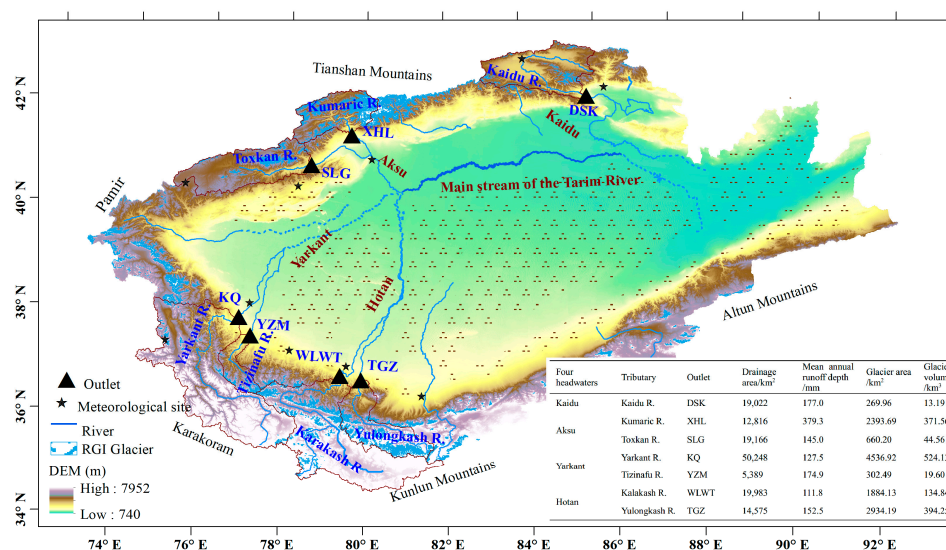


**Figure 1.** The location of the headwaters in the Tarim River Basin, along with the corresponding meteorological and hydrological stations. The mountainous runoff from its four headwaters (namely, Kaidu River, Aksu River, Yarkant River, and Hotan River) flows into the mainstream, forming the Tarim River. The four headwaters, along with their corresponding tributaries and outlets, are listed. The glacier area and estimated glacier volume were derived from the first China Glacier Inventory and the images were taken around 1965 [15].

During the historical period, it is widely believed that the increase in temperature led to an increase in glacier melt and snowmelt water. This and the increased precipitation have jointly resulted in increased runoff [5,16]. Future changes in runoff for mountainous rivers have drawn attention from scholars in the context of global warming. However, estimating future runoff changes comes with significant uncertainty in terms of magnitude and direction (Table 1). There are several reasons for this uncertainty. Firstly, the Tarim River Basin covers a vast area with varying sources of water vapor and hydroclimatic conditions. Prediction of future climate will vary depending on geographical locations and geomorphological features. Low-resolution global circulation models (GCMs) often struggle to accurately represent spatial variations of climatic conditions. Secondly, mountainous rivers are influenced by multiple factors such as rainfall, glaciers, snowpack, and permafrost processes. These hydrological processes are challenging to depict or understand due to limited observations and the spatial heterogeneity of geographical characteristics. Some models even exclude glacier dynamic processes and rely solely on observed streamflow data for calibration. Thirdly, most studies have focused on the Kaidu River, while paying less attention to the Yarkant and Hotan Rivers. Previous research suggests that future river

runoff may exhibit an increasing trend in the near future (until 2050). However, in the long term (end of the 21st century), the runoff may show a decreasing trend, which could increase the future risk in the water system of the Tarim River Basin [17–20].

**Table 1.** Future runoff changes in the Tarim River Basin as reported in the literature.

Study Area	Methodology	Main Conclusions
The three headwaters of the Tarim River (namely, the Aksu, Yarkant, and Hotan Rivers)	Combination of 1 GCM and 1 hydrological model (VIC-3L)	Under the A2 and B2 scenarios, runoff in 2020–2025 showed a slightly decreasing trend compared to 2000–2005, with an increase in spring and a decrease in winter [21].
	Combination of 3 GCMs (CSIRO, ECHAM, GFDL) and 1 hydrological model (VIC-3L)	Under the A1B, A2, and B1 scenarios, runoffs in 2046–2065 and 2081–2100 show a decreasing trend compared to 1981–2000, with an increase in winter and spring and a decrease in summer [22].
	Combination of four GCMs in CMIP5 and improved SWAT model	Under the RCP2.6, RCP4.5, and RCP8.5 scenarios, runoff is projected to increase by 15~45% in 2066 to 2095 compared to 1966–1995 [22].
	Combination of two glacio-hydrological models with output of eight GCMs	River discharge in the Aksu River catchments is projected to initially increase by about 20% with subsequent decreases of up to 20%. Discharge in the Hotan and Yarkant catchments is projected to increase by 15–60% towards the end of the century [19].
The mainstream of the Tarim River	Multi-objective calibrated SWAT-Glacier model forces by bias-corrected CORDEX outputs	In the period of 2006–2035, under RCP4.5 and RCP8.5 scenarios, runoff is projected to increase by 3.2% and 3.9%, respectively, compared to the reference period (this study).
	Combination of HadGEM2-ES and MIKE SHE	Under RCP2.6 scenario, runoff is expected to reduce (−5.04~−0.6%) in 2021–2050 compared with 1981–2004, with greater reduction under RCP8.5 than RCP2.6 [23].
	Combination of 5 GCMs and the advanced Bayesian Neural Network	Under the RCP8.5 scenario, runoff is projected to increase by 9.12%, 15.33%, and 21.04%, in the 2020s, 2050s, and 2080s, respectively, compared to 1980~2009 [24].
	Combination of HadCM3 and SWAT, with two downscaling methods (SDSM and STARS)	Under the A2 (B2) scenario, runoff is expected to decrease (remain basically unchanged) after the 2020s compared to 1961–2010 [25].
Kaidu River	Combination of 2 GCMs (CanESM and BNU-ESM) and SDHydro	Under the RCP2.6, RCP4.5 and RCP8.5, scenarios, runoff is projected to increase or remain basically unchanged during 2006 to 2100, with the dominant peak flow shifting from summer to spring [26].
	Combination of 21 GCMs (CMIP5) and SWAT model	Under the RCP4.5 and RCP8.5 scenarios, runoff is expected to reduce by 12.5% [3.4~26%] and 18% [7~38%], respectively, in 2080–2099 compared to 1986~2005 [18].
	Combination of 36 GCMs and a lump model and a distributed MIKE-SHE model	In the period of 2046–2064, runoff is projected to decrease slightly in July and August (−6.2~3.7%) compared to 1979–1998 [27].
	Combination of one GCM and improved SWAT model	Under the RCP4.5 scenario, runoff is expected to show a significant downward trend with a reduction in the proportion of glacier meltwater in 2066–2095 compared to 1966–1995 [28].
	Combination of 1 GCM and SWAT model	Under the RCP2.6, RCP4.5, RCP6.0, and RCP8.5 scenarios, runoff is projected to reduce by 21.5–40.0% in 2041–2080 relative to 1961–2000, with a decrease in winter and an increase in spring [29].
	Combination of GCMs (CMIP5) and BPANN	Runoff is projected to show a significant increasing trend from 2016 to 2050 at a rate of 0.4 billion m <sup>3</sup> per decade [30].

Table 1. Cont.

Study Area	Methodology	Main Conclusions
Aksu River (namely, the Kumaric and Toxkan Rivers)	Combination of GCM (CMIP5) and BPANN	From 2016 to 2050, runoff of the Kumaric and Toxkan Rivers is projected to increase significantly at rates of 3.5 and $1.0 \times 10^8 \text{ m}^3$ per decade, respectively [30].
	Combination of 9 GCMs, 2 RCMs, and improved WASA model (incorporated with the $\Delta h$ -approach)	Runoff of the Kumaric River will change by 29%, 18%, and $-5\%$ in the 2020s, 2050s, and 2080s, respectively, with a significant increase in spring and early summer compared to 1971–2000. The glacier area is projected to decrease by 7–58% by 2050 compared with 2000 [17].
Yarkant River	Combination of 5 GCMs and the improved WASA model (with snowmelt module)	The Kumaric River is expected to transition from being primarily influenced by snow/glacier melt in the early 21st century to a rainfall-dominated regime by the later 21st century [31].
	Combination of multiple GCMs and a degree day model	Under the A1B, A2 and B1 scenarios, annual glacier runoff is projected to increase until 2050, with total runoff over glacierized areas increasing by about 13–35% during 2011–2050 relative to that during 1961–2006 [32].
	Combination of GCM and GHRU-SWAT	Runoff is expected to increase by 30% [2% to 62%] by 2100 compared to 1966–1995. The proportion of glacier meltwater is projected to increase in the upcoming decades but decline in the long term [28].
	22 GCMs in CMIP5 and VIC-Glacier model	Under the RCP8.5 scenario, glacier melt dominates the increases in runoff with a relative increase of $29 \pm 11\%$ in the first half of the 21st century compared to the period of 1971–2000 [1].

To address the spatial variability in hydrometeorological conditions in the alpine areas, we utilized the high-resolution regional climate model (RCM) of the Coordinated Regional Downscaling Experiment (CORDEX) program conducted in Central Asia. In order to assess future changes in runoff, a glacier dynamic module was incorporated into the SWAT-Glacier model. The SWAT-Glacier model was then forced by the bias-corrected RCM outputs to predict alterations in runoff of the four headwaters (namely, the Kaidu River, Aksu River, Yarkant River, and the Hotan River). The objective of this study is to provide a scientific foundation for future water resource management and development plans of the Tarim River Basin.

## 2. Data and Methodology

This study utilized the “CORDEX-bias correction-SWAT-glacier” model chain to simulate future changes in runoff. Specifically, the high-resolution climate dataset of CORDEX [33] was firstly bias-corrected. Then, the corrected climate data were used to force the distributed hydrological model SWAT-Glacier. Finally, the changes in runoffs of the future periods (2006–2035 (P2), 2036–2065 (P3), and 2066–2095 (P4)) were compared with the historical period (1976–2005) in the headwaters of the Tarim River (Figure 2).

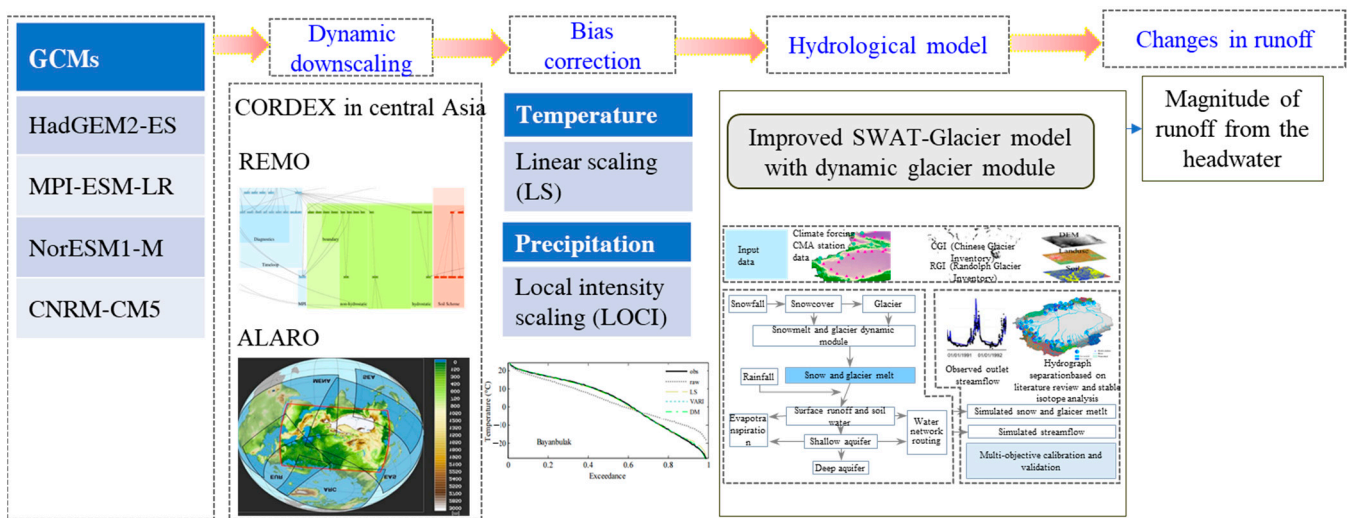


**Figure 2.** Flow chart of the computation procedure.

2.1. RCMs

The low resolution of the Global Climate Model (GCM) hinders its ability to accurately capture the intricate characteristics of climate change in high mountainous regions. To address this limitation, Regional Climate Models (RCMs) offer a viable approach by providing a better representation of the complex topography of the area. In this study, we utilized the outputs of RCMs from CORDEX, an important sub-program of the World Climate Research Program (WCRP). The spatial resolution of CORDEX data ranges from 22 km to 44 km, enabling a more accurate reflection of the climate change patterns in the inland region of Central Asia. For our analysis, we selected a total of 6 combinations of GCMs and RCMs to obtain future climate change information of the Tarim River Basin under the RCP4.5 and RCP8.5 scenarios (Table 2).

**Table 2.** The regional climate models (RCMs) used in this study.

GCMs	RCM-Institute	RCMs	Spatial/Temporal Resolution	Scenarios
CNRM-CERFACS-CNRM-CM5	RMIB-Ugent	ALARO-0	22 km, day	RCP4.5, RCP8.5
MOHC-HadGEM2-ES	GERICS	REMO2015	22 km, day	RCP8.5
MPI-M-MPI-ESM-LR	GERICS	REMO2015	22 km, day	RCP8.5
NCC-NorESM1-M	GERICS	REMO2015	22 km, day	RCP8.5
MOHC-HadGEM2-ES	BOUN	RegCM4-3	44 km, day	RCP4.5, RCP8.5
MPI-M-MPI-ESM-MR	BOUN	RegCM4-3	44 km, day	RCP4.5, RCP8.5

2.2. Bias Correction Method

Considering the significant bias present in the outputs of RCMs, it is essential to apply bias correction techniques before utilizing them for water resources research. In this study, we performed bias correction on temperature and precipitation data using the Linear Scaling (LS) and Local Intensity Scaling (LOCI) methods, respectively. The bias correction was conducted on a daily basis for the period from 1975 to 2005 [34]. Further details on the application of the bias correction methods can be found in the work of Fang et al. [34].

2.3. SWAT-Glacier Model Extended with Glacier Dynamic Module

To simulate and predict future runoff in the alpine watershed, we incorporated the glacier dynamic module into the original version of the SWAT model (Soil and Water Assessment Tool) and developed the SWAT-Glacier distributed hydrological model for each headwater [35,36]. The SWAT-Glacier introduces four ice melting parameters, namely the maximum/minimum ice melting rate  $gmfmx$  and  $gmfmn$ , the temperature lag factor

$L_{gla}$ , and the melting base temperature  $Gmtmp$ , which are all subject to calibration. Similar to the snowmelt calculation in SWAT, the glacier melt is calculated using the degree day method [37], a widely accepted approach for accounting glacier melt processes. The theoretical foundation of the degree day method has been extensively described in previous studies [38] and proven effective in simulating glacier meltwater in alpine catchment areas [35,36]. Additional details on the SWAT-Glacier model can be found in [35,36]. It is important to note that due to the large number of glaciers and their complex movement [39,40], the SWAT-Glacier model does not consider glacier movement such as surges.

#### 2.4. Model Setup and Multi-Objective Calibration

The SWAT-Glacier model was constructed for each catchment within the seven of the Tarim River (Figure 1). For each catchment, subbasins were generated based on flow direction and extracted river network using the Digital Elevation Model (DEM). Subsequently, these subbasins were further divided into hydrological response units (HRUs) based on land use and soil information. The numbers of subbasins derived from the seven catchments ranged from 19 to 33. Original glacier area data were used as input for the SWAT-Glacier model. We calibrated the SWAT-Glacier model using the second-generation multi-objective evolutionary algorithm ( $\epsilon$ -NSGAII) with three objective functions: Nash–Sutcliffe efficiency coefficient (NS), the relative changes in glacier area during the simulation period ( $BIAS_G$ ), and the balance between snow accumulation and snowmelt plus snow sublimation ( $BIAS_S$ ). The  $\epsilon$ -NSGAII algorithm is known for its effectiveness and reliability in finding the global optimal parameters of hydrological models [41,42].

$$NS = 1 - \frac{\sum_{i=1}^n (Y_i^{obs} - Y_i^{sim})^2}{\sum_{i=1}^n (Y_i^{obs} - Y^{mean})^2} \quad (1)$$

$$BIAS_G = \begin{cases} 0, & \left| \delta_{gla\_area}^{sim} - \delta_{gla\_area}^{obs} \right| \leq 0.05 \\ \left| \delta_{gla\_area}^{sim} - \delta_{gla\_area}^{obs} \right| - 0.05, & \text{else} \end{cases} \quad (2)$$

$$BIAS_S = \begin{cases} 0, & 0.9 \leq \frac{snowfall}{snowmelt+sublimation} \leq 1.1 \\ \left| \frac{snowfall}{snowmelt+sublimation} - 1 \right| - 0.1, & \text{else} \end{cases} \quad (3)$$

where  $NS$  is the Nash–Sutcliffe coefficient of daily streamflow;  $Y_i^{obs}$  and  $Y_i^{sim}$  are the  $i$ th observed and simulated daily streamflow, respectively;  $Y^{mean}$  is the average of the observed streamflow;  $n$  is the number of observations.  $BIAS_G$  is the bias between the simulated ( $\delta_{gla\_area}^{sim}$ ) and observed ( $\delta_{gla\_area}^{obs}$ ) changes in glacier area over the entire simulation period. For the Kaidu River Basin, according to the first and second China Glacier Inventory, the glacier area reduced from 270.02 km<sup>2</sup> to 183.05 km<sup>2</sup>, resulting in  $C_{gla\_area}^{obs}$  being  $-32.2\%$  during 1968 to 2008 [15]. Similarly, for the Kumaric and Toxkan Rivers, the  $C_{gla\_area}^{obs}$  values are  $-26.7\%$  and  $-23.3\%$ , respectively, during 1975 to 2016 [43]. For the Yarkant and Tizinafu Rivers, the  $C_{gla\_area}^{obs}$  values are  $-18.0\%$  and  $-27\%$  during 1976–2010 [15]. Lastly, for the Karakashi and Yulongkashi Rivers, the  $C_{gla\_area}^{obs}$  values are  $-17.8\%$  and  $-7.0\%$  during 1970–2010 [15]. If the disparity between simulated and observed changes in glacier area is within 5%,  $BIAS_G$  is set at 0 to account for uncertainties in the literature records. The  $NS$  denotes how well the simulated streamflow matches the observation, with higher values indicating more reliable simulations.  $BIAS_G$  measures the average deviation between the simulated and observed changes in glacier area.  $BIAS_S$  represents the snow balance during the simulation period to avoid snow tower [44]. The model calibration was conducted based on observed meteorological variables. The calibration period for  $BIAS_G$  and  $BIAS_S$  aligns with the observed period of glacier area change. The calibration period for daily streamflow is 2001–2005, while the validation period extends from 2006 to 2011. In future predictions, it is assumed that the parameters related to land use and soil will remain

unchanged. The bias-corrected daily precipitation and maximum/minimum temperature were used to force the SWAT-Glacier model to estimate future changes in streamflow. Other meteorological factors such as solar radiation, wind speed, and relative humidity were held unchanged as they were found to have a small impact on streamflow based on the Sobols' sensitivity analysis [34].

### 3. Results

#### 3.1. Evaluation of Corrected Precipitation and Temperature

Figure 3 displays the exceedance probability curves and time series of the observed, raw RCM-simulated, and the bias-corrected temperature and precipitation data in each catchment. In comparison to the observations, the raw RCM simulation deviates significantly. The applied bias correction methods greatly improve the raw RCM-simulated temperature and precipitation. The results show that the following: (1) For air temperature, nearly all GCM-RCMs underestimate the mountainous air temperature. The corrected air temperature shows good agreement with the observed temperature in terms of both frequency and time series indices. (2) For precipitation, all GCM-RCMs overestimate the precipitation in mountainous areas. Nevertheless, the corrected precipitation effectively mimics the monthly mean value and also the number of wet days (precipitation amount  $\geq 0.1$  mm/day).

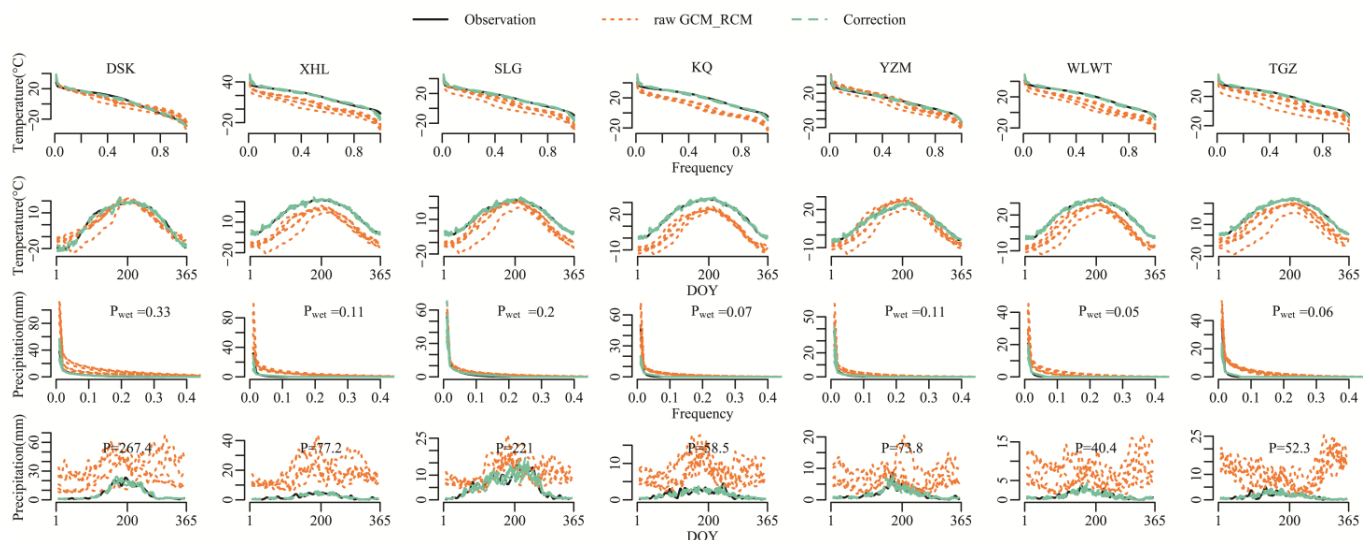


**Figure 3.** The exceedance probability curves and the time series of the observed, RCM-simulated, and bias-corrected temperature and precipitation averaged in the headstreams of the Tarim River during the period of 1976–2005. For precipitation, the wet day proportion ( $P_{wet}$ ) and mean annual precipitation are presented.

#### 3.2. Evaluation of SWAT-Glacier Model

Figure 4 illustrates the exceedance probability curves (flow duration curves) and time series plots of the observed streamflow (“obs”), simulated streamflows using observed meteorological inputs (“sim-obs”), and corrected RCM outputs (“sim-cor”). Overall, the SWAT-Glacier model driven by the observed meteorological data (“sim-obs”) successfully reproduces the observed probability curves and the time series. The parameter set used for this simulation is listed in Table S1. However, the performance of SWAT-Glacier forced by the corrected CORDEX outputs (“sim-cor”) is slightly inferior but still acceptable. These simulations generally match the observations for probabilities larger than 0.05. However, they fail to correctly mimic the peak flow, resulting in an underestimation of 10–32% in Catchment DSK, XHL SLG, and YZM, while other catchments show overestimations of 17–32%. Regarding the hydrograph, SWAT-Glacier effectively simulates summer peak flow and winter low flow. However, due to the model’s inability to account for the influence of

permafrost on catchment hydrology, it fails to capture the quick recession in late autumn in Catchment KQ (Figure 4) [45].

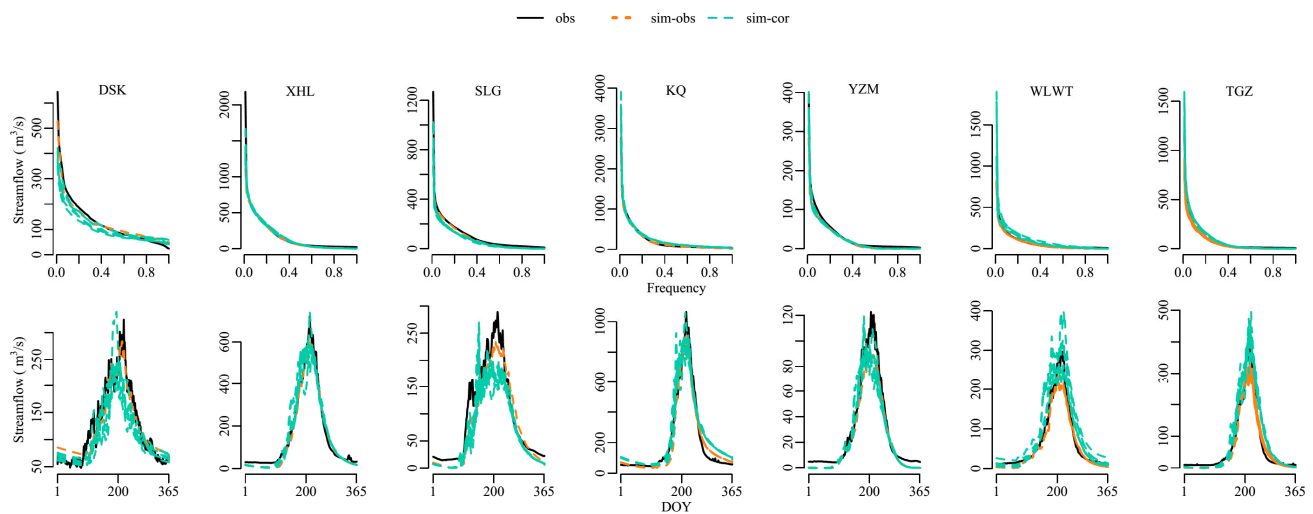


**Figure 4.** The exceedance plots and hydrographs of daily streamflows of observation, simulations using the SWAT-Glacier model forced by observed meteorological data (“sim-obs”), and bias-corrected RCM outputs (“sim-cor”). Each line represents the averaged hydrograph during the calibration period.

Table 3 presents the evaluation metrics for the simulations forced by both the observed and corrected CORDEX meteorological variables. The daily NS efficiency coefficients of the simulations using observed meteorological data (“sim-obs”) ranged from 0.56 to 0.81 during the calibration period and from 0.51 to 0.74 during the validation period. The monthly NS coefficients ranged from 0.69 to 0.87, indicating satisfactory performance of the SWAT-Glacier model. Regarding  $BIAS_G$ , the model successfully simulated the changes in glacier area throughout the simulation period. When driven by the corrected CORDEX data (“sim-cor”), the simulation performance slightly decreased, but the monthly NS efficiency coefficients remained 0.60 for all tributaries. The biases in simulated glacier area changes ( $BIAS_G$ ) were within 10%, except for Catchment WLWT (Table 3). In terms of snow balance, the SWAT-Glacier model effectively balanced snow accumulation and snowmelt/sublimation, with optimal  $BIAS_S$  values of 0 for most simulations.

**Table 3.** Model performance of the SWAT-Glacier model in the headwaters of the Tarim River.

River System	Hydrological Stations	SWAT-Glacier Driven by Observed Meteorological Data (“sim-obs”)				SWAT-Glacier Driven by Corrected CORDEX Data (“sim-cor”)		
		Calibration Period		Validation Period		NS (Monthly)	$BIAS_G$	$BIAS_S$
		NS (Daily)	NS (Monthly)	NS (Daily)	NS (Monthly)			
Kaidu	DSK	[0.81, 0.81]	[0.89, 0.89]	[0.74, 0.74]	[0.83, 0.83]	[0.68, 0.31]	[0.00, 0.00]	[0.00, 0.00]
	XHL	[0.75, 0.75]	[0.87, 0.87]	[0.76, 0.76]	[0.87, 0.87]	[0.78, 0.68]	[0.00, 0.08]	[0.00, 0.08]
Aksu	SLG	[0.53, 0.53]	[0.66, 0.66]	[0.54, 0.54]	[0.69, 0.69]	[0.60, 0.50]	[0.00, 0.00]	[0.00, 0.00]
	KQ	[0.76, 0.75]	[0.87, 0.87]	[0.76, 0.76]	[0.87, 0.87]	[0.73, 0.48]	[0.08, 0.26]	[0.00, 0.20]
Yarkant	YZM	[0.56, 0.56]	[0.72, 0.72]	[0.56, 0.56]	[0.72, 0.72]	[0.67, 0.56]	[0.07, 0.46]	[0.00, 0.00]
	WLWT	[0.58, 0.56]	[0.75, 0.74]	[0.58, 0.58]	[0.77, 0.76]	[0.77, 0.47]	[0.45, 0.50]	[0.00, 0.39]
Hotan	TGZ	[0.68, 0.66]	[0.82, 0.78]	[0.68, 0.64]	[0.81, 0.77]	[0.75, 0.53]	[0.10, 0.17]	[0.00, 0.00]

### 3.3. Future Climate Change in the Tarim River Basin

Under the RCP4.5 and RCP8.5 scenarios, temperatures in the Tarim River Basin are projected to continue rising throughout the 21st century, with a higher increase under

the RCP8.5 scenario compared to RCP4.5. By the middle of the 21st century (2036–2065), temperatures are expected to rise by  $1.22 \pm 0.72$  °C compared to the historical period (1976–2005) under the RCP8.5 scenario. The southern Tianshan Mountains such as the Kaidu and Aksu River are projected to experience a higher temperature increment (e.g., 1.39 °C) compared to the northern Kunlun Mountains (e.g., 1.21 °C in the Yarkant and Hotan River Basins). Towards the end of the 21st century, the temperature increment is estimated to reach approximately  $4.27 \pm 2.59$  °C. There are also variations among the GCM-RCM models, with NorESM-REMO and CNRM-CM5-ALARO predicting a warmer climate.

In the 21st century, precipitation is also expected to increase in the Tarim River Basin (Figure 5). Compared to the historical period (1976–2005), average precipitation is projected to increase by  $3.81 \pm 14.72$  mm and  $20.53 \pm 27.65$  mm during the periods 2036–2065 and 2066–2095, respectively. The greatest increase in precipitation is anticipated in the northern slope of the Kunlun Mountains (e.g., the KQ, YZM, WLWT, and TGZ River Basin), while the increase in the southern slope of the Tianshan Mountains (e.g., DSK River Basin) is expected to be more subtle. From 2006 to 2035, the increment in precipitation under RCP4.5 is smaller than that under RCP8.5, but this trend reverses after the 2050s, with a lower precipitation increment under RCP8.5 compared to RCP4.5. It is important to note that with increased precipitation, the variability of precipitation is also expected to increase, as indicated by the standard deviation rising from 0.96 mm during 1975–2005 to 1.30 mm in 2066–2095.

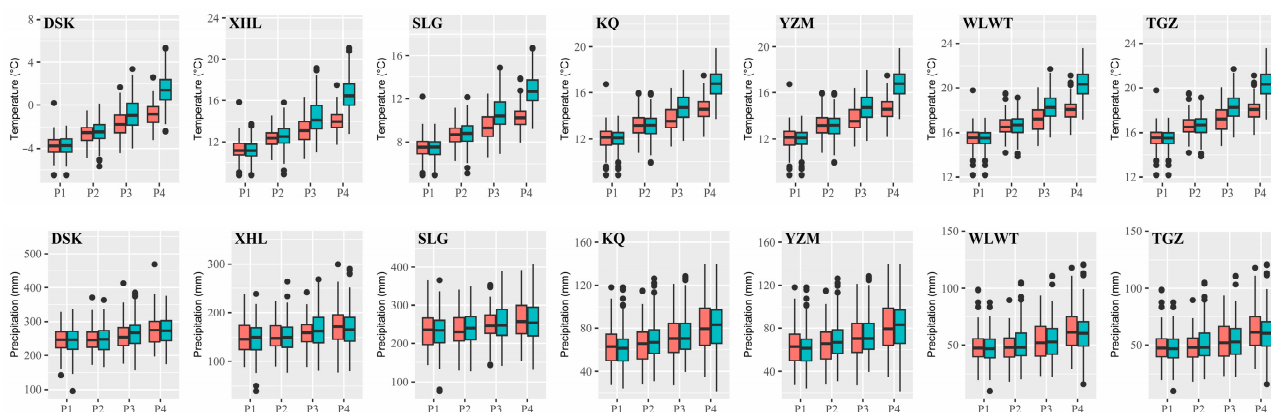


**Figure 5.** Variations of annual temperature and precipitation in the headwaters of the Tarim River under RCP4.5 and RCP8.5 scenarios. The red and green boxes indicate the RCP4.5 and RCP8.5 scenarios. Among them, P1, P2, P3, and P4 refer to 1976–2005, 2006–2035, 2036–2065, and 2066–2095, respectively.

### 3.4. Future Runoff Changes in the Headwaters

Figure 6 illustrates the projected changes in runoff for each tributary in the Tarim River Basin. For the Kaidu River (DSK), there is a slight decrease in runoff, with a decrease of 2.3% and 7.8% under the RCP4.5 and RCP8.5 scenarios, respectively, in the near term (before 2035). For the Aksu Rivers (XLS and SLG), there is a subtle increase in runoff, with an increment of 3.6% and 3.9% under the RCP4.5 and RCP8.5 scenarios, respectively, between 2006 and 3035. By the end of the 21st century, the increase in runoff is projected to be 17.6% and 9.3% for the two scenarios.

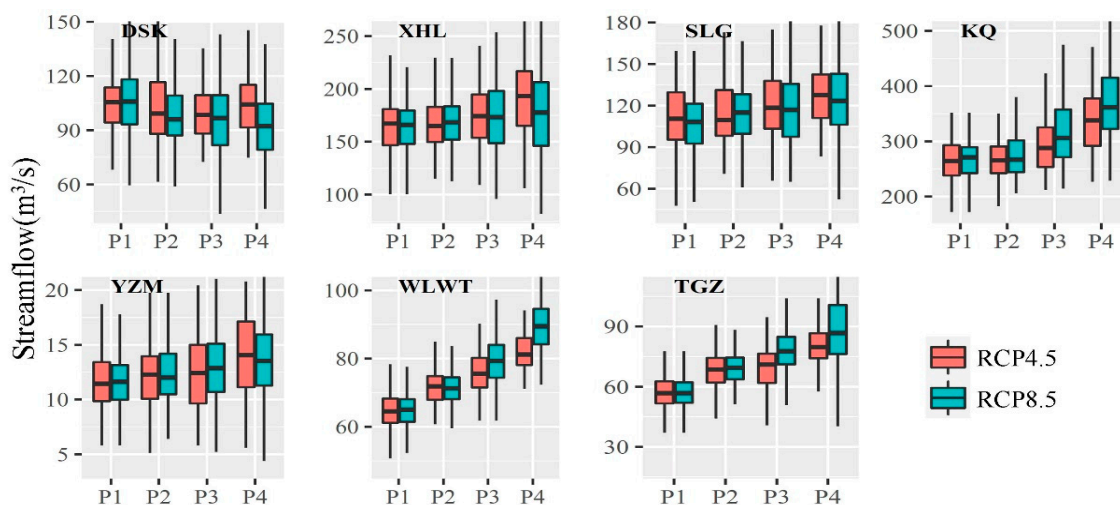


**Figure 6.** Runoff changes in the headwaters of the Tarim River Basin under RCP4.5 and RCP8.5 scenarios. The whiskers show the 5% and 95% quantiles of the streamflow.

For the Yarkant River (KQ and YZM), which has large-scale glaciers in its upper reaches with an estimated glacier volume of 624 km<sup>3</sup> in 2010 [46], it is expected that runoff will increase significantly under future warming scenarios due to increased glacial meltwater recharge and precipitation. The projected runoff increase is 10.0% and 17.0% under the RCP4.5 and RCP8.5 scenarios, respectively, during the period 2036–2065. By the end of the 21st century, the runoff in the Yarkant River Basin is expected to increase by 26.4% and 38.0% under the two emission scenarios. For the Hotan River (WLWT and TGZ), the runoff is projected to increase by 14.4% and 15.6% under the two scenarios in 2016–2035 and by 32.2% and 45% in 2066–2095 (Table 4 and Figure 6). Interestingly, due to the continued increase in precipitation, the runoff of the north slope of the Kunlun Mountains is not expected to reach a tipping point.

**Table 4.** Variations in runoffs predicted using the “CORDEX-bias correction-SWAT-glacier” model chain in the Tarim River Basin ( $\times 10^8$  m<sup>3</sup>).

Headwater System	RCP4.5				RCP8.5			
	1976–2005	2006–2035	2036–2065	2066–2095	1976–2005	2006–2035	2036–2065	2066–2095
Kaidu River	33.1	32.3	31.7	33.1	33.4	30.8	30.6	29.0
Aksu River	86.0	89.3	92.4	100.2	85.1	89.6	92.9	95.9
Yarkant River	88.3	88.3	97.0	111.4	89.0	90.8	103.9	122.0
Hotan River	38.6	44.0	45.8	51.2	38.6	44.4	49.5	55.7
Total	246.0	253.8	266.9	296.0	246.1	255.6	276.9	302.7

The seasonal changes in runoff patterns vary significantly among different tributaries (Figure 7). In rivers where glacier meltwater accounts for a small proportion (e.g., less than 10% in DSK and less than 20% in SLG, Fang et al., 2018), the seasonal changes in runoff are characterized by an increase in spring and a decrease in summer. On the other hand, rivers that receive a large proportion of their recharge from glacier meltwater, as well as those located in the northern Kunlun Mountainous region (e.g., XHL, KQ, WLWT, and TGZ), experience a notable increase in summer runoff due to the combined effects of summer ice melting and increased precipitation.

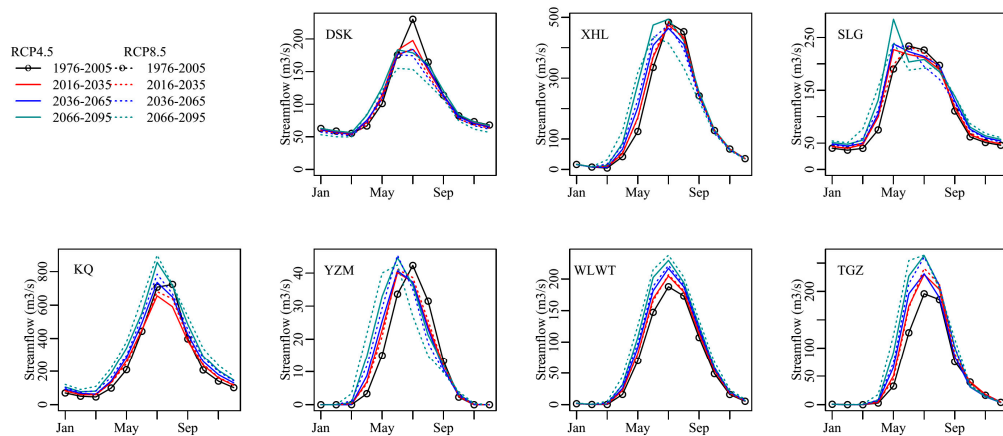


Figure 7. Seasonal changes in runoffs of the Tarim River Basin under RCP4.5 and RCP8.5 scenarios.

Figure 8 aggregates the absolute changes of runoffs in the headwaters of the Tarim River through the 21st century under the RCP4.5 and RCP8.5 scenarios. The average annual runoff in the headwaters of the Tarim River was approximately  $246.0 \times 10^8 \text{ m}^3$  during the period from 1976 to 2005. Under the RCP4.5 scenario, there is a projected increase of 3.2% in runoff during the period from 2006 to 2035, corresponding to an additional  $7.84 \times 10^8 \text{ m}^3$ . Similarly, under the RCP8.5 scenario, there is an estimated increase of 3.9% in runoff during the same period, amounting to an extra  $9.56 \times 10^8 \text{ m}^3$ . The most significant changes are anticipated to occur between 2065 and 2095, particularly under the RCP8.5 scenario, where a substantial increment of 23% in runoff is expected.

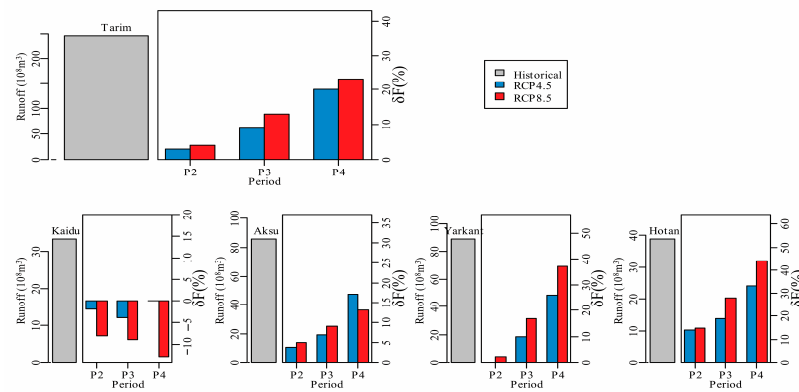


Figure 8. Historical runoff (1976–2005) of the Tarim River Basin and its relative changes ( $\Delta F$ ) under RCP4.5 and RCP8.5 scenarios in the 21st century (P2: 2006–2035, P3: 2036–2065, P4: 2066–2095). The mean annual runoff and its relative changes of the four headwaters are also plotted.

#### 4. Discussion

##### 4.1. Comparison with Existing Studies

The future runoff of the Kaidu River is expected to exhibit a fluctuating and decreasing trend, which aligns with previous studies [18,25,28,29] but differs from predictions based on the advanced Bayesian Neural Network (BNN) approach [24]. The inconsistency in projected runoff changes is likely due to variations in climate models, as the largest uncertainty in the "climate model-bias correction-hydrological model" chain stems from climate models themselves. Moreover, some hydrological models lack a glacier meltwater module or assume constant glacier area without considering glacier ablation, leading to differences in runoff predictions. However, considering the high simulation accuracy of the Kaidu River, with an NS efficiency coefficient of 0.63 and well-reproduced glacier area changes, the future changes in runoff for the Kaidu River are highly reliable.

For the Aksu River Basin with a glacier area of 13,567 km<sup>2</sup> [43], future runoff is projected to increase, consistent with results obtained from the BPANN neural network model [30]. Some studies have also indicated that the Aksu River's runoff will reach a tipping point around 2040 [17,19] or continue to decrease steadily [47].

For the Yarkant and Hotan Rivers, runoff is expected to experience a significant increase during the 21st century, consistent with findings from various hydrological models and climate data. For instance, a modified distributed hydrological model (HEC-HMS) predicts a runoff increase of 10.62–19.2% during 2021–2049 and 36.69–70.4% in 2071–2099 [48]. Large-scale glacier evolution models like OGGM [11], the well-established Variable Infiltration Capacity (VIC) model coupled with a degree day glacier melt algorithm [1], and a modified SWAT model [28] also project substantial runoff increases. Specifically, SWIM-G and WASA simulations consistently show continuously increasing annual mean discharge [19]. Precipitation in the Yarkant and Hotan River Basins is expected to exhibit a significant upward trend, with predicted increases of 60–140 mm and 59–150 mm during 2022 to 2050 under SSP245 and SSP585 scenarios [4,49]. These rivers may shift from being dominated by glacier meltwater to being dominated by rainfall and snowmelt water due to increased rainfall extremes [50–52]. Consequently, the volatility of the runoff will increase, the intra- and inter-annual allocation will be more complex, and water resource vulnerability will increase [53].

For alpine catchments, the most notable change in other hydrological variables is the decline in glacier area [2,54]. Taking the Kumaric River as an example, changes in snowmelt, snow water equivalent, glacier area, and glacier melt are demonstrated in Figure 9. The snow water equivalent shows a clear decline during the 21st century, consistent with the concerns raised by Kraaijenbrink et al. [13]. As expected, the glacier area exhibits a continuous declining trend, while glacier melt initially increases and then decreases. Notably, the reductions in snow water equivalent and glacier area are more pronounced under the RCP8.5 scenario compared to RCP4.5.

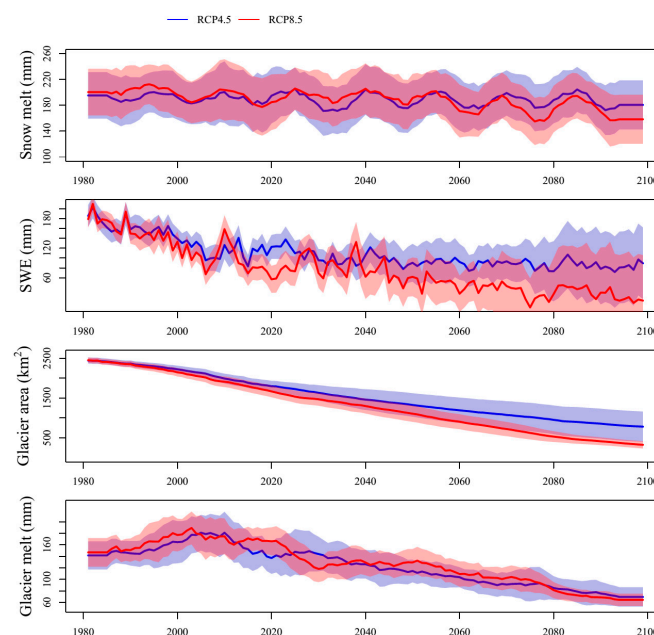


**Figure 9.** Future changes in snowmelt, snow water equivalent, glacier area, and glacier melt under RCP4.5 and RCP8.5 in the Kumaric River Basin. The shaded area indicates the standard deviation of the ensemble simulations.

#### 4.2. Uncertainties and Limitations

The assessment of future runoff changes suffers from uncertainties that can arise from various sources, including GCMs, bias correction methods, and hydrological models. Previous studies have shown that the uncertainty caused by climate models is significant [18].

In this study, multiple high-resolution RCM outputs were utilized to represent climate conditions. The use of multiple climate models has been proven to provide a more comprehensive synthesis of future projections compared to relying on a single model [4,55]. However, accurately quantifying mountainous precipitation poses challenges, as some rain sites may not be effective in harsh environments. Despite efforts to reduce uncertainty in the hydrological SWAT-Glacier model through multi-objective calibration and validation procedures that narrow down parameter sets, these procedures only constrain the runoff and glacier area. Other variables remain unconstrained, introducing the possibility of “equifinality.”

Furthermore, there are certain limitations that need to be addressed. This study assumes no changes in land use. However, with increasing temperature, precipitation, and CO<sub>2</sub> levels, transpiration patterns may change, potentially influencing the hydrological cycle and the accuracy of predicted runoff changes [12,56,57]. It should also be noted that the projected runoff changes presented in this study are derived from limited hydrological and climate models.

#### 4.3. Implications and Future Adaptations

Over the past two decades, there has been a significant increase in runoff in the headwaters of the Tarim River, presenting a valuable opportunity for water utilization in this arid region [16]. On one hand, it is crucial to utilize the increasing runoff efficiently to support regional development. On the other hand, measures need to be implemented to mitigate flood risks associated with the rise in hydrological extremes. Examples of such measures include the construction of mountainous reservoirs and the establishment of a connected water system.

Considering the magnitude of uncertainties in future projections, it is necessary to enhance data collection and improve related modeling techniques [20]. This is particularly important when it comes to accurately estimating precipitation in alpine regions. Therefore, we recommend four measures to enhance the projection of future runoff: (1) Efforts should be made to deepen our understanding of complex hydrological processes, aiming to make hydrological models as close to reality as possible. (2) Enhance the precision of glacier volume estimation and implement high-resolution monitoring of glaciers using cutting-edge techniques. (3) Provide more detailed information on the accumulation and ablation of each glacier while considering the balance between precision and computational burden. (4) Develop a network for remote sensing-based monitoring of precipitation magnitude, pattern, and extremes in mountainous regions.

## 5. Conclusions

Global warming has had a profound impact on climatic conditions, including temperature and precipitation patterns, resulting in changes in glaciers, snow meltwater, and runoff in the Tarim River Basin. This study utilizes climate simulation data from the CORDEX program in Central Asia to force the distributed hydrological SWAT-Glacier model and analyze future runoff changes in the headwaters of the Tarim River. The following conclusions can be drawn:

- (1) Temperature is projected to continue rising in the future, accompanied by increased precipitation with great fluctuations in the Tarim River Basin. Under the RCP8.5 scenario, the temperature is expected to increase by  $1.22 \pm 0.72$  °C during the period 2036–2065. The rate of the temperature increase is greater in the southern slope of the Tianshan Mountains compared to the northern slope of the Kunlun Mountains. In comparison to the historical period (1976–2005), precipitation is anticipated to increase by an average of  $3.81 \pm 14.72$  mm and  $20.53 \pm 27.65$  mm during the periods 2036–2065 and 2066–2095, respectively.
- (2) Overall, runoff is projected to increase in the headwaters of the Tarim River. However, the Kaidu River is expected to experience a decreasing trend in runoff, while other rivers exhibit an increasing trend. Regarding annual distribution, earlier peak

flows are projected in the Kaidu River, and increased summer flows are expected in the Yarkant and Hotan Rivers. These changes pose significant challenges for water resource management, considering the existing water scarcity in irrigation and the heightened risk of summer floods. Given the increased water variability and hydrological extremes associated with climate change, it is crucial to implement special measures to enhance water management. This study provides valuable insights for the economic and social development of the entire basin.

**Supplementary Materials:** The following supporting information can be downloaded at: <https://www.mdpi.com/article/10.3390/rs15163922/s1>. Table S1: Model parameter set in the SWAT-Glacier model in the headwaters of the Tarim River.

**Author Contributions:** Conceptualization and writing, G.F. and Z.L.; methodology, G.F.; model validation and results analysis, Y.C., W.L., X.Z. and Q.Z. All authors have read and agreed to the published version of the manuscript.

**Funding:** This research was supported by the Tianshan Talent Program of Xinjiang, China (2022TSY-CCX0042), the National Natural Science Foundation of China (42071046,42130512), and the Western Young Scholar of the Chinese Academy of Sciences (2022-XBQNXX-002). The authors gratefully acknowledge the Youth Innovation Promotion Association of the Chinese Academy of Sciences (2019431) and the Youth Talent Lifting Project of Xinjiang Province.

**Data Availability Statement:** The data that support the findings of this study are available from the Xinjiang Tarim River Basin Management Bureau. We gratefully acknowledge the contributors of the first and second China Glacier Inventory.

**Conflicts of Interest:** The authors declare no conflict of interest.

## References

1. Su, F.; Pritchard, H.D.; Yao, T.; Huang, J.; Ou, T.; Meng, F.; Sun, H.; Li, Y.; Xu, B.; Zhu, M. Contrasting fate of western Third Pole's water resources under 21st century climate change. *Earth Future* **2022**, *10*, e2022EF002776. [CrossRef]
2. Huss, M.; Hock, R. Global-scale hydrological response to future glacier mass loss. *Nat. Clim. Chang.* **2018**, *8*, 135–140. [CrossRef]
3. Greve, P.; Kahil, T.; Mochizuki, J.; Schinko, T.; Satoh, Y.; Burek, P.; Fischer, G.; Tramberend, S.; Burtscher, R.; Langan, S.; et al. Global assessment of water challenges under uncertainty in water scarcity projections. *Nat. Sustain.* **2018**, *1*, 486–494. [CrossRef]
4. IPCC. *Climate Change 2022: Impacts, Adaptation, and Vulnerability*; IPCC: Cambridge, UK; New York, NY, USA, 2022; pp. 1–3056.
5. Chen, Y. *Water Resources Research in Northwest China*; Springer Science & Business Media: Berlin/Heidelberg, Germany, 2014.
6. Bhattacharya, A.; Bolch, T.; Mukherjee, K.; King, O.; Menounos, B.; Kapitsa, V.; Neckel, N.; Yang, W.; Yao, T. High Mountain Asian glacier response to climate revealed by multi-temporal satellite observations since the 1960s. *Nat. Commun.* **2021**, *12*, 4133. [CrossRef]
7. Huang, J.; Su, F.; Yao, T.; Sun, H. Runoff regime, change, and attribution in the upper Syr Darya and Amu Darya, central Asia. *J. Hydrometeorol.* **2022**, *23*, 1563–1585. [CrossRef]
8. Khanal, S.; Lutz, A.F.; Kraaijenbrink, P.D.; van den Hurk, B.; Yao, T.; Immerzeel, W.W. Variable 21st century climate change response for rivers in High Mountain Asia at seasonal to decadal time scales. *Water Resour. Res.* **2021**, *57*, e2020WR029266. [CrossRef]
9. Pritchard, H.D. Asia's shrinking glaciers protect large populations from drought stress. *Nature* **2019**, *569*, 649–654. [CrossRef]
10. Immerzeel, W.W.; Van Beek, L.P.; Bierkens, M.F. Climate change will affect the Asian water towers. *Science* **2010**, *328*, 1382–1385. [CrossRef]
11. Zhao, H.; Su, B.; Lei, H.; Zhang, T.; Xiao, C. A new projection for glacier mass and runoff changes over High Mountain Asia. *Sci. Bull.* **2023**, *68*, 43–47. [CrossRef]
12. Zhou, S.; Yu, B.; Lintner, B.R.; Findell, K.L.; Zhang, Y. Projected increase in global runoff dominated by land surface changes. *Nat. Clim. Chang.* **2023**, *13*, 1–8. [CrossRef]
13. Kraaijenbrink, P.D.A.; Stigter, E.E.; Yao, T.; Immerzeel, W.W. Climate change decisive for Asia's snow meltwater supply. *Nat. Clim. Chang.* **2021**, *11*, 591–597. [CrossRef]
14. Masood, M.; Yeh, P.J.F.; Hanasaki, N.; Takeuchi, K. Model study of the impacts of future climate change on the hydrology of Ganges–Brahmaputra–Meghna basin. *Hydrol. Earth Syst. Sci.* **2015**, *19*, 747–770. [CrossRef]
15. Shi, Y.; Liu, C.; Kang, E. The glacier inventory of China. *Ann. Glaciol.* **2009**, *50*, 1–4. [CrossRef]
16. Chen, Y.; Li, Z.; Xu, J.; Shen, Y.; Xing, X.; Xie, T.; Li, Z.; Yang, L.; Xi, H.; Zhu, C.; et al. Changes and Protection Suggestions in Water Resources and Ecological Environment in Arid Region of Northwest China. *Bull. Chin. Acad. Sci.* **2023**, *38*, 385–393.
17. Duethmann, D.; Menz, C.; Jiang, T.; Vorogushyn, S. Projections for headwater catchments of the Tarim River reveal glacier retreat and decreasing surface water availability but uncertainties are large. *Environ. Res. Lett.* **2016**, *11*, 054024. [CrossRef]

18. Fang, G.; Yang, J.; Chen, Y.; Li, Z.; De Maeyer, P. Impact of GCM structure uncertainty on hydrological processes in an arid area of China. *Hydrol. Res.* **2018**, *49*, 893–907. [[CrossRef](#)]
19. Wortmann, M.; Duethmann, D.; Menz, C.; Bolch, T.; Huang, S.; Jiang, T.; Kundzewicz, Z.W.; Krysanova, V. Projected climate change and its impacts on glaciers and water resources in the headwaters of the Tarim River, NW China/Kyrgyzstan. *Clim. Chang.* **2022**, *171*, 30. [[CrossRef](#)]
20. Bolch, T.; Duethmann, D.; Wortmann, M.; Liu, S.; Disse, M. Declining glaciers endanger sustainable development of the oases along the Aksu-Tarim River (Central Asia). *Int. J. Sustain. Dev. World Ecol.* **2022**, *29*, 209–218. [[CrossRef](#)]
21. Liu, Z.; Xu, Z.; Huang, J.; Charles, S.P.; Fu, G. Impacts of climate change on hydrological processes in the headwater catchment of the Tarim River basin, China. *Hydrol. Process* **2010**, *24*, 196–208. [[CrossRef](#)]
22. Liu, Z.; Xu, Z.; Fu, G.; Yao, Z. Assessing the hydrological impacts of climate change in the headwater catchment of the Tarim River basin, China. *Hydrol. Res.* **2013**, *44*, 834–849. [[CrossRef](#)]
23. Ban, C.; Tao, H.; Dong, Y.; Zhao, C. Simulation of Daily Runoff Process in the Mainstream Area of the Tarim River Under Future Climate Scenario. *Arid. Zone Res.* **2018**, *35*, 770–778.
24. Ren, W.; Yang, T.; Shi, P.; Xu, C.-Y.; Zhang, K.; Zhou, X.; Shao, Q.; Ciais, P. A probabilistic method for streamflow projection and associated uncertainty analysis in a data sparse alpine region. *Glob. Planet Chang.* **2018**, *165*, 100–113. [[CrossRef](#)]
25. Xu, C.; Zhao, J.; Deng, H.; Fang, G.; Tan, J.; He, D.; Chen, Y.; Chen, Y.; Fu, A. Scenario-based runoff prediction for the Kaidu River basin of the Tianshan Mountains, Northwest China. *Environ. Earth Sci.* **2016**, *75*, 1126. [[CrossRef](#)]
26. Zhang, F.; Li, L.; Ahmad, S. Streamflow pattern variations resulting from future climate change in middle Tianshan Mountains region in China. In Proceedings of the World Environmental and Water Resources Congress 2017, Sacramento, CA, USA, 21–25 May 2017; pp. 437–446.
27. Liu, T.; Willems, P.; Pan, X.L.; Bao, A.M.; Chen, X.; Veroustraete, F.; Dong, Q.H. Climate change impact on water resource extremes in a headwater region of the Tarim basin in China. *Hydrol. Earth Syst. Sc.* **2011**, *15*, 3511–3527. [[CrossRef](#)]
28. Luo, Y.; Wang, X.; Piao, S.; Sun, L.; Ciais, P.; Zhang, Y.; Ma, C.; Gan, R.; He, C. Contrasting streamflow regimes induced by melting glaciers across the Tien Shan–Pamir–North Karakoram. *Sci. Rep.* **2018**, *8*, 16470. [[CrossRef](#)] [[PubMed](#)]
29. Huang, Y.; Ma, Y.; Liu, T.; Luo, M. Climate change impacts on extreme flows under IPCC RCP scenarios in the mountainous Kaidu watershed, Tarim River basin. *Sustainability* **2020**, *12*, 2090. [[CrossRef](#)]
30. Wang, C.; Xu, J.; Chen, Y.; Bai, L.; Chen, Z. A hybrid model to assess the impact of climate variability on streamflow for an ungauged mountainous basin. *Clim. Dynam.* **2018**, *50*, 2829–2844. [[CrossRef](#)]
31. Huang, J. *Analysis of Stream Flow Composition in Glacierized Inland River Basin—Case Study from Aksu River Basin*; University of Chinese Academy of Sciences: Beijing, China, 2019; pp. 1–210.
32. Zhang, S.; Gao, X.; Zhang, X.; Hagemann, S. Projection of glacier runoff in Yarkant River basin and Beida River basin, Western China. *Hydrol. Process* **2012**, *26*, 2773–2781. [[CrossRef](#)]
33. Giorgi, F.; Jones, C.; Asrar, G.R. Addressing climate information needs at the regional level: The CORDEX framework. *World Meteorol. Organ. (WMO) Bull.* **2009**, *58*, 175.
34. Fang, G.; Yang, J.; Chen, Y.; Zammit, C. Comparing bias correction methods in downscaling meteorological variables for a hydrologic impact study in an arid area in China. *Hydrol. Earth Syst. Sc.* **2015**, *19*, 2547–2559. [[CrossRef](#)]
35. Fang, G.; Yang, J.; Chen, Y.; Li, Z.; Ji, H.; De Maeyer, P. How Hydrologic Processes Differ Spatially in a Large Basin: Multisite and Multiobjective Modeling in the Tarim River Basin. *J. Geophys. Res. Atmos.* **2018**, *123*, 7098–7113. [[CrossRef](#)]
36. Ji, H.; Fang, G.; Yang, J.; Chen, Y. Multi-Objective Calibration of a Distributed Hydrological Model in a Highly Glacierized Watershed in Central Asia. *Water* **2019**, *11*, 554. [[CrossRef](#)]
37. Neitsch, S.; Arnold, J.; Kiniry, J. *Soil and Water Assessment Tool Theoretical Manual*; Grassland Soil Water Research Laboratory: Temple, TX, USA, 2002.
38. Hock, R. Temperature index melt modelling in mountain areas. *J. Hydrol.* **2003**, *282*, 104–115. [[CrossRef](#)]
39. Zhang, Q.; Xu, C.-Y.; Tao, H.; Jiang, T.; Chen, Y.D. Climate changes and their impacts on water resources in the arid regions: A case study of the Tarim River basin, China. *Stoch. Environ. Res. Risk Assess.* **2010**, *24*, 349–358. [[CrossRef](#)]
40. Liu, S.; Ding, Y.; Shanguan, D.; Zhang, Y.; Li, J.; Han, H.; Wang, J.; Xie, C. Glacier retreat as a result of climate warming and increased precipitation in the Tarim river basin, northwest China. *Ann. Glaciol.* **2006**, *43*, 91–96. [[CrossRef](#)]
41. Kollat, J.B.; Reed, P.M. Comparing state-of-the-art evolutionary multi-objective algorithms for long-term groundwater monitoring design. *Adv. Water Resour.* **2006**, *29*, 792–807. [[CrossRef](#)]
42. Yang, J.; Castelli, F.; Chen, Y. Multiobjective sensitivity analysis and optimization of distributed hydrologic model MOBIDIC. *Hydrol. Earth Syst. Sci.* **2014**, *18*, 4101–4112. [[CrossRef](#)]
43. Zhang, Q.; Chen, Y.; Li, Z.; Li, Y.; Xiang, Y.; Bian, W. Glacier changes from 1975 to 2016 in the Aksu River Basin, Central Tianshan Mountains. *J. Geogr. Sci.* **2019**, *29*, 984–1000. [[CrossRef](#)]
44. Freudiger, D.; Kohn, I.; Seibert, J.; Stahl, K.; Weiler, M. Snow redistribution for the hydrological modeling of alpine catchments. *WIREs Water* **2017**, *4*, e1232. [[CrossRef](#)]
45. Gao, H.; Han, C.; Chen, R.; Feng, Z.; Wang, K.; Fenicia, F.; Savenije, H. Diagnosing the impacts of permafrost on catchment hydrology: Field measurements and model experiments in a mountainous catchment in western China. *Hydrol. Earth Syst. Sci. Discuss.* **2021**, *2021*, 1–31. [[CrossRef](#)]

46. Feng, T.; Liu, S.; Xu, J.; Guo, W.; WEI, J.; Zhang, Z. Glacier change of the Yarkant River basin from 1968 to 2009 derived from the First and Second Glacier Inventories of China. *J. Glaciol. Geocryol.* **2015**, *37*, 1–13. [[CrossRef](#)]
47. Bliss, A.; Hock, R.; Radić, V. Global response of glacier runoff to twenty-first century climate change. *J. Geophys. Res. Earth Surf.* **2014**, *119*, 717–730. [[CrossRef](#)]
48. Xiang, Y.; Wang, Y.; Chen, Y.; Zhang, Q. Impact of Climate Change on the Hydrological Regime of the Yarkant River Basin, China: An Assessment Using Three SSP Scenarios of CMIP6 GCMs. *Remote Sens.* **2022**, *14*, 115. [[CrossRef](#)]
49. Liu, Q.; Liu, Y.; Niu, J.; Gui, D.; Hu, B.X. Prediction of the Irrigation Area Carrying Capacity in the Tarim River Basin under Climate Change. *Agriculture* **2022**, *12*, 657. [[CrossRef](#)]
50. Li, Y.; Chen, Y.; Wang, F.; He, Y.; Li, Z. Evaluation and projection of snowfall changes in High Mountain Asia based on NASA's NEX-GDDP high-resolution daily downscaled dataset. *Environ. Res. Lett.* **2020**, *15*, 104040. [[CrossRef](#)]
51. Chen, F.; Xie, T.; Yang, Y.; Chen, S.; Chen, F.; Huang, W.; Chen, J. Discussion of the “warming and wetting” trend and its future variation in the drylands of Northwest China under global warming. *Sci. China Earth Sci.* **2023**, *66*, 1241–1257. [[CrossRef](#)]
52. Ombadi, M.; Risser, M.D.; Rhoades, A.M.; Varadharajan, C. A warming-induced reduction in snow fraction amplifies rainfall extremes. *Nature* **2023**, *619*, 305–310. [[CrossRef](#)]
53. Wang, T.; Zhao, Y.; Xu, C.; Ciais, P.; Liu, D.; Yang, H.; Piao, S.; Yao, T. Atmospheric dynamic constraints on Tibetan Plateau freshwater under Paris climate targets. *Nat. Clim. Chang.* **2021**, *11*, 219–225. [[CrossRef](#)]
54. Hugonnet, R.; McNabb, R.; Berthier, E.; Menounos, B.; Nuth, C.; Girod, L.; Farinotti, D.; Huss, M.; Dussaillant, I.; Brun, F. Accelerated global glacier mass loss in the early twenty-first century. *Nature* **2021**, *592*, 726–731. [[CrossRef](#)]
55. Wang, N.; Sun, F.B.; Wang, H.; Liu, W.B. Effects of cryospheric hydrological processes on future flood inundation and the subsequent socioeconomic exposures in Central Asia. *Environ. Res. Lett.* **2022**, *17*, 124020. [[CrossRef](#)]
56. Betts, R.A.; Boucher, O.; Collins, M.; Cox, P.M.; Falloon, P.D.; Gedney, N.; Hemming, D.L.; Huntingford, C.; Jones, C.D.; Sexton, D.M.H.; et al. Projected increase in continental runoff due to plant responses to increasing carbon dioxide. *Nature* **2007**, *448*, 1037–1041. [[CrossRef](#)] [[PubMed](#)]
57. Mastrotheodoros, T.; Pappas, C.; Molnar, P.; Burlando, P.; Manoli, G.; Parajka, J.; Rigon, R.; Szeles, B.; Bottazzi, M.; Hadjidoukas, P.; et al. More green and less blue water in the Alps during warmer summers. *Nat. Clim. Chang.* **2020**, *10*, 155–161. [[CrossRef](#)]

**Disclaimer/Publisher's Note:** The statements, opinions and data contained in all publications are solely those of the individual author(s) and contributor(s) and not of MDPI and/or the editor(s). MDPI and/or the editor(s) disclaim responsibility for any injury to people or property resulting from any ideas, methods, instructions or products referred to in the content.